Isolated molecular dopants in pentacene observed by scanning tunneling microscopy

Sieu D. Ha* and Antoine Kahn
Department of Electrical Engineering, Princeton University, Princeton, New Jersey 08544, USA
(Received 11 August 2009; published 13 November 2009)

Doping is essential to the control of electronic structure and conductivity of semiconductor materials. Whereas doping of inorganic semiconductors is well established, doping of organic molecular semiconductors is still relatively poorly understood. Using scanning tunneling microscopy, we investigate, at the molecular scale, surface and subsurface tetrafluoro-tetracyanoquinodimethane *p*-dopants in the prototypical molecular semiconductor pentacene. Surface dopants diffuse to pentacene vacancies and appear as negatively charged centers, consistent with the standard picture of an ionized acceptor. Subsurface dopants, however, have the effect of a positive charge, evidence that the donated hole is localized by the parent acceptor counterion, in contrast to the model of doping in inorganic semiconductors. Scanning tunneling spectroscopy shows that the electron potential energy is locally lowered near a subsurface dopant feature, in agreement with the localized hole model.

DOI: 10.1103/PhysRevB.80.195410 PACS number(s): 73.61.Ph, 68.55.Ln, 68.37.Ef

I. INTRODUCTION

The control of doping in semiconductors is essential to modern electronics and many subfields of solid-state physics. Electrical doping in organic devices has progressed significantly in the past decade.[1–5] However, in spite of appreciable development of doping in organic molecular materials, the theory and understanding of the processes involved remain in infancy, relative to inorganic semiconductors. In the latter case, the physics of doping has been well established for many years. In organic materials, however, the general effects of a dopant in a host matrix are not fundamentally understood, and consequently, selecting effective dopants is not fully rationalized. Accurate models are still needed to account for the energy levels of an ionized dopant in an organic film, the range of the associated potential, the degree of (de)localization of the released carrier, and many other properties. In this work, we present a molecular-scale investigation of a dopant in an organic host matrix. We use scanning tunneling microscopy and spectroscopy (STM/STS) to visualize the effects of surface dopants, subsurface dopants, and associated donated carriers in an organic film. By studying organic doping on such a scale, we hope to elucidate the intimate interaction between host and dopant, which has not been well explained to date.

In order to study doping at the molecular level, we chose the model system of pentacene doped with tetrafluoro-tetracyanoquinodimethane (F_4-TCNQ). Pentacene is perhaps the most extensively studied material in organic electronics due to its relatively high carrier mobility.[6] The acceptor molecule F_4-TCNQ has been shown to be an efficient *p*-dopant in a number of hole-transport materials.[2,7] It is also a *p*-dopant in pentacene, as its electron affinity (5.24 eV) is greater than the ionization energy of the host (5.0 eV).[2,8,9] Electrical doping is confirmed by recent current-voltage measurements performed in our laboratory, which show an increase in conductivity of more than two orders of magnitude upon doping pentacene with 0.5% F_4-TCNQ.[10] In the present work, we grow, by thermal evaporation, well ordered multilayer films of pentacene on the (001) surface of bismuth (Bi) on Si(111). Pentacene molecules have been shown to align on Si(111)/Bi(001) in an upright phase from the first monolayer (ML) and exhibit a Frank–van der Merwe epitaxial growth.[11] These films are an ideal crystalline template for the incorporation and investigation of single dopants. F_4-TCNQ is deposited by thermal evaporation to investigate surface doping, and dopants are subsequently buried under an additional pentacene ML to investigate bulk doping. Occupied and unoccupied state microscopy and spectroscopy are then performed to probe the electronic properties of observed features.

II. EXPERIMENT

All samples were prepared in an ultra-high vacuum (UHV) chamber with base pressure below 5.0×10^{-11} Torr. Approximately 200 Å of Bi were deposited by thermal evaporation on a 7×7 reconstructed Si(111) surface and converted to the Bi(001) crystal structure by annealing at about 400 K for 30 min.[12] Approximately 3–4 ML of pentacene were subsequently deposited on Bi(001). This thickness of pentacene is sufficient to decouple the electronic structure of the semimetallic substrate from the density of states (DOS) of the surface molecular layer.[13] Samples were analyzed in an interconnected UHV chamber ($p\sim4.0\times10^{-11}$ Torr) using a room-temperature STM, and images were processed with WSxM software from Nanotec Electronica, Spain.[14] STS spectra were averaged over thousands of *I-V* traces, and DOS curves were extracted according to the method of Wagner *et al.*[15]

III. RESULTS AND DISCUSSION

An STM image of the 3–4 ML pentacene film on Bi(001) is presented in Fig. 1(a). The large scale image shows that the film has high structural order. As stated above, the molecules are in an upright configuration. A schematic of the molecular arrangement is shown in Fig. 1(b). As per the diagram, each bright spot in Fig. 1(a) corresponds to a single pentacene molecule. The molecular orientation is confirmed

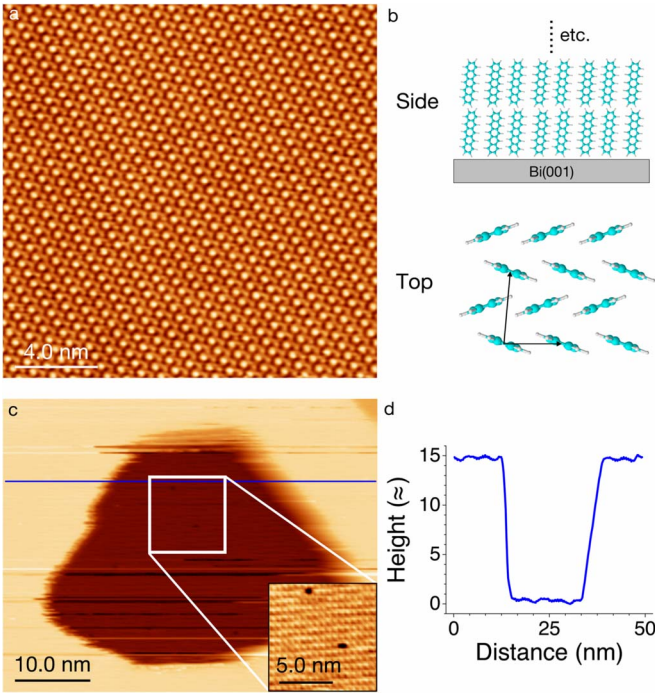

FIG. 1. (Color online) (a) STM image of Si(111)/Bi(001)/3–4 ML pentacene showing high crystalline order (V_s=−2.2 V, I_t =40 pA, 18.0×18.0 nm^2). (b) Schematic diagram of side and top views of pentacene thin film in (a). (c) STM image of similarly prepared sample as in (a), with hole in topmost layer (V_s= −2.0 V, I_t=30 pA, 50.0×39.2 nm^2). Inset: Zoom-in of hole area, showing clear pentacene order (10.0×10.0 nm^2). (d) Line profile agrees well with length of pentacene molecule, illustrating that pentacene film is in an upright configuration.

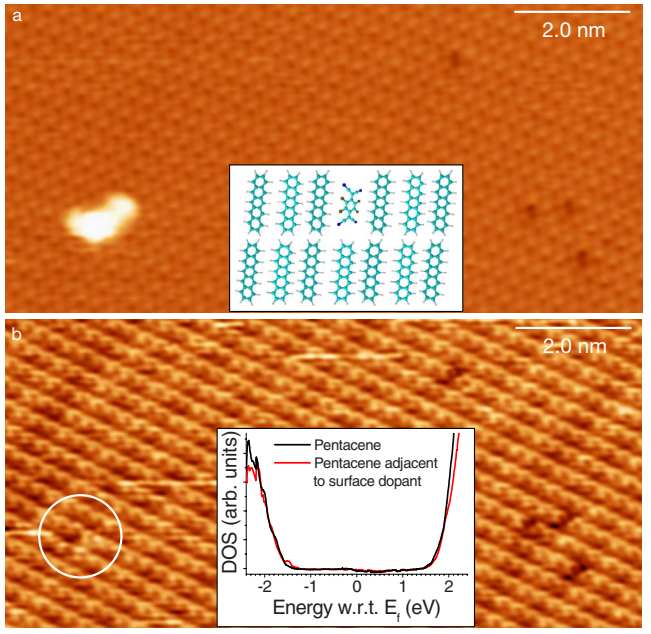

FIG. 2. (Color online) (a) Occupied states STM image with effect of ionized dopant (V_s=−2.3 V, I_t=40 pA, 22.6 ×11.0 nm^2). Inset: Side view schematic of F_4-TCNQ located in a pentacene vacancy site. Not to scale. (b) Unoccupied states STM image of same area as in (a), but without visible effect of surface dopant (V_s=+1.5 V, I_t=30 pA, 22.6×11.0 nm^2). Circle marks vacancy defect observed in the same area as bright feature of (a). Inset: DOS plots obtained from STS, recorded with the tip over pentacene molecules adjacent to a surface dopant (red) and over pentacene molecules far from a surface dopant (black). The DOS show no significant energy level shift, as expected.

by a line profile of the image in Fig. 1(c), which shows a hole in the topmost pentacene layer. The line profile [Fig. 1(d)] reveals that the hole is 14.4 Å deep, in good agreement with the length of pentacene.[16] The inset of Fig. 1(c) shows that within the hole, ordered pentacene is observable, which confirms that the film is indeed multilayer.

A. Surface dopants

Following the investigation of pristine pentacene, a small amount of F_4-TCNQ was deposited in order to study dopant molecules located at the surface of the film. STM images of the surface of F_4-TCNQ-doped pentacene are shown in Fig. 2(a) (occupied states) and Fig. 2(b) (unoccupied states). The specific array of defects on the right-hand sides of both images gives clear evidence that the images were recorded on the same area of the pentacene surface. The defects are vacancy sites in the crystalline pentacene layer, which are observed in undoped pentacene films [Fig. 1(c) inset] and which facilitate tracking of the scanned area. The bright feature in the lower left corner of Fig. 2(a) is an effect attributed to F_4-TCNQ since no such features are observed before F_4-TCNQ exposure and since the density of these features scales with increasing dopant coverage. This bright feature is noticeably absent in Fig. 2(b). The appearance and disappearance of the feature is not the result of unintentional molecular manipulation by the STM tip. The bias-dependent behavior is robust through many polarity switches over several hours of sample scanning, as illustrated in Fig. 3 for a different area of the sample. This implies that the bright features in Figs. 2(a), 3(b), and 3(c) correspond to an electronic effect related to F_4-TCNQ, but are not the physical dopant molecules themselves. Recall that in typical constant-current mode, STM images are a combination of the surface topography as well as the surface DOS (occupied or unoccupied, depending on bias conditions).[17] Topographical features such as step edges and admolecules are observable regardless of sample bias. Features that show strong bias dependence, however, are due to significant local DOS changes at the surface. Since bias conditions exist for which the features in Figs. 2(a), 3(b), and 3(c) cannot be observed, they must be due to electronic DOS effects related to F_4-TCNQ and not topographical signatures of the dopant themselves.

While we claim that the aforementioned bright features are not physical molecules but electronic effects of F_4-TCNQ, the dopant molecules must still be accounted for in order to cause the local changes in DOS. Close inspection of Fig. 2(b) (circle) and Figs. 3(a) and 3(d) reveals that a vacancy defect is observed in unoccupied states in the position where a bright feature is observed in occupied states, suggesting that the F_4-TCNQ molecules are located inside the pentacene vacancy sites. This accounts for the absence of a topographical contribution attributed to F_4-TCNQ, particu-

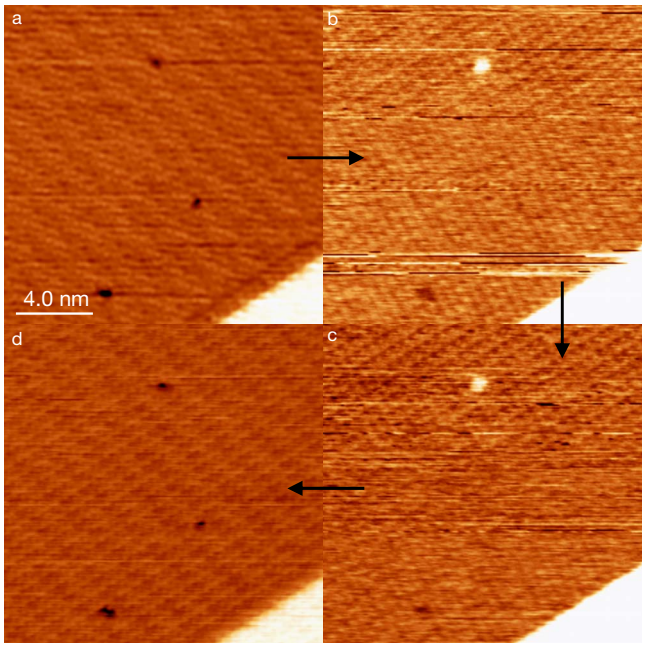

FIG. 3. (Color online) Chronological sequence of STM images showing strict bias dependence of the bright feature related to a surface dopant. Images demonstrate that the bright feature is due to a local change in DOS, not a physical adsorbate. All images are 16.5×16.5 nm^2. From upper left counterclockwise, sample biases are (a) V_s=+1.8 V, (b) V_s=−2.0 V, (c) V_s=−2.0 V, and (d) V_s= +1.8 V.

larly in unoccupied states images. If instead the dopant was adsorbed on the surface of pentacene, it would likely be observable in both occupied and unoccupied state imaging, due to its physical structure. At higher dopant coverage, large clusters are observed in STM and growth is nonepitaxial, which implies that F_4-TCNQ molecules diffuse on the surface of pentacene and form aggregates. At low coverage, as in Figs. 2 and 3, a neutral F_4-TCNQ molecule likely diffuses on the pentacene surface until it encounters and fills a vacancy. Such a substitutional configuration [Fig. 2(a) inset] offers greater cofacial alignment, which enhances the π-orbital interaction between pentacene and F_4-TCNQ molecules and is more energetically favorable with respect to the case of a dopant molecule on the host surface, where interaction with the upright pentacene molecules would be weak.[18]

The contrast between the occupied and unoccupied states images originates from the DOS of the ionized molecule. From energy level considerations, F_4-TCNQ is expected to capture an electron from the host pentacene and release a hole. Density functional theory (DFT) calculations have shown that the highest occupied and lowest unoccupied molecular orbitals (HOMO, LUMO) of F_4-TCNQ both split upon ionization (F_4-TCNQ$\rightarrow F_4$-TCNQ$^-$).[19] Of the four new levels, two HOMO- and one LUMO-derived states are occupied and lower in energy than the sample Fermi level. Only one unoccupied LUMO-derived level remains above the Fermi level, and the gap separating it from the next (LUMO+1) level is large (>2 eV). Therefore, there are more states that contribute to tunneling in occupied states imaging than in unoccupied states imaging, resulting in a bright feature in Fig. 2(a) that is not apparent in Fig. 2(b). Moreover, depending on the exact position of the Fermi level within the F_4-TCNQ$^-$ bandgap, the one unoccupied LUMO-derived state may not be accessed by STM without relatively high sample bias. Indeed, images have been recorded at higher positive sample bias, e.g., +2.2 V, in which the bright feature becomes visible in unoccupied states imaging as well (not shown here). Note that, when combined with the donor molecule α-sexithiophene in a charge-transfer complex, F_4-TCNQ$^-$ exhibits similar bias dependence in STM imaging as presented here.[20] These observations therefore demonstrate that the features shown in Figs. 2 and 3 are due to the anion F_4-TCNQ$^-$. Finally, note that the size and shape of the bright localized feature is expected to vary with tip shape and potential distribution around the ionized dopant.

B. Subsurface dopants

In order to study the bulk behavior of a molecular dopant, an additional monolayer of pentacene is deposited on the surface-doped Bi(001)/pentacene/F_4-TCNQ sample. STM images of a region of the host/dopant/host sandwich structure [Fig. 4(a) inset] are shown in Figs. 4(a) and 4(b). The occupied states image [Fig. 4(a)] contains two large depression features, which appear as bright hillocks in the unoccupied states image [Fig. 4(b)]. As with the surface dopant, the hillock/depression features are not observed in undoped films, and the bias-dependent appearance is not due to unintentional manipulation of adsorbates by the STM tip. The features are due to an electronic effect of imaging under different bias conditions rather than a physical protrusion or indentation. As a result, we attribute the features in Fig. 4 to the effect of subsurface dopants. The relative size difference between features is likely due to a varying number of subsurface dopant molecules.

Varying the sample bias, e.g., from −2.0 V to −1.4 V [Figs. 4(c) and 4(d), respectively], further demonstrates that the features in Figs. 4(a) and 4(b) are the signature of subsurface species. The depression marked by a circle in Fig. 4(c) is virtually undetectable in Fig. 4(d). In the latter, the pentacene structure appears wholly undisturbed around the same area as in Fig. 4(c). This demonstrates that: (1) the features in Figs. 4(a) and 4(b) are caused by dopants which are beneath the topmost pentacene layer and (2) such subsurface dopants do not appreciably disrupt the lattice structure of the host.

As stated in the introduction, the energetics of the pentacene-F_4-TCNQ system and the *I-V* measurements on doped vs. undoped pentacene clearly demonstrate that doping occurs via ionization of the *p*-dopant and release of a hole. Yet, the signature of the F_4-TCNQ subsurface dopant, which appears in STM as a hillock in unoccupied states and as a depression in occupied states images, is opposite to that of a subsurface *p*-type dopant in an inorganic semiconductor.[21,22] In the latter case, the feature imaged by STM is a *negatively* charged ionized acceptor atom, which locally increases the potential energy for electrons at the surface. This reduces (enhances) the tip-induced band bending

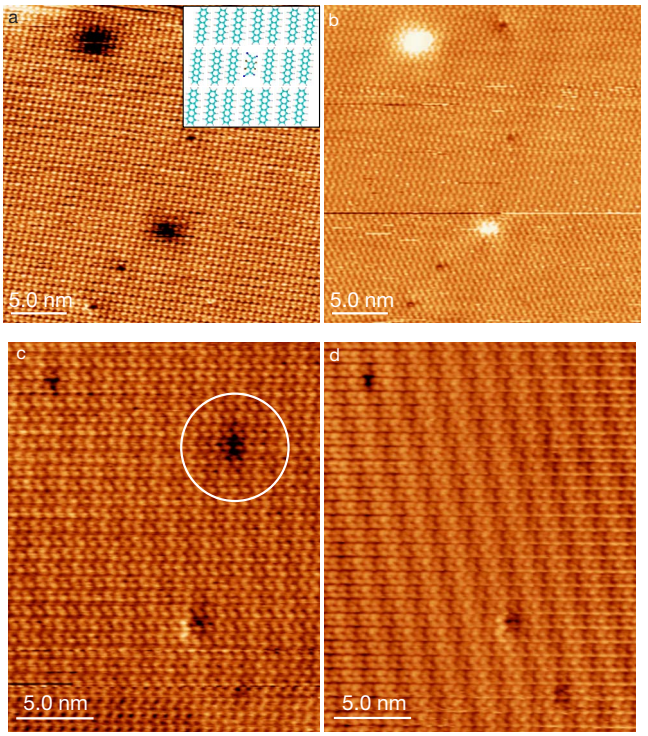

FIG. 4. (Color online) (a) Occupied states STM image showing depression effect of subsurface dopants (V_s=−1.6 V, I_t =40 pA, 28.1×28.1 nm^2). Inset: Side view diagram of pentacene/F_4-TCNQ/pentacene structure. (b) Unoccupied states STM image showing hillock effect of subsurface dopants (V_s= +2.0 V, I_t=30 pA, 28.1×28.1 nm^2). (c) STM image at relatively high bias showing depression effect of subsurface dopant (circle) (V_s=−2.0 V, I_t=30 pA, 16.0×20.0 nm^2). (d) STM image of same area as (c), in which effect of subsurface dopant is nearly unobservable and pentacene lattice appears unperturbed, confirming subsurface position of F_4-TCNQ dopant (V_s= −1.4 V, I_t=30 pA, 16.0×20.0 nm^2).

in occupied (unoccupied) states imaging, resulting in an increase (decrease) of the overlap between semiconductor and tip states active in tunneling, thus producing a hillocklike (depressionlike) feature in the negative (positive) bias image.[22] On the other hand, the apparent inverse behavior of subsurface dopants in the pentacene–F_4-TCNQ system suggests that the hillock/depression feature in Figs. 4(a) and 4(b) is instead the effect of a *positively* charged species. This situation is diagrammed in Figs. 5(a) and 5(b). A positively charged species confined near the surface will locally decrease the surface potential energy for electrons, which in turn enhances (reduces) the "band sloping" caused by the tip-induced field in occupied (unoccupied) states imaging. The result, which is opposite to the above inorganic case, is to decrease the tunneling current for occupied states imaging [Fig. 5(a)], and to increase the tunneling current for unoccupied states imaging [Fig. 5(b)]. This model is consistent with the present observations, suggesting that the hillock/depression feature is the signature of a positive charge around the ionized acceptor. The positive charge is attributed to the hole released by the acceptor molecule, but localized by the ionized dopant potential.

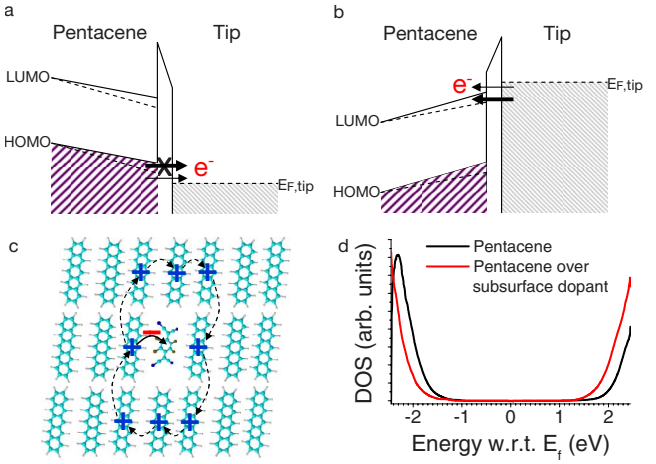

FIG. 5. (Color online) (a) and (b) Energy level diagrams for occupied (unoccupied) states STM imaging, illustrating potential lowering due to localized positive surface charge, which reduces (increases) the occupied (unoccupied) DOS involved in tunneling, causing a depression (hillock) in imaging. (c) Side view diagram illustrating subsurface dopant effect at room temperature. An electron is captured by F_4-TCNQ (solid line). The donated hole is localized near the ionized dopant site but hops between pentacene molecules (dashed lines). (d) DOS plots obtained from STS, recorded with the tip over pentacene molecules influenced by a subsurface dopant [red (gray in print version)] and over pentacene molecules far from dopant features (black).

The localization of the donated hole in F_4-TCNQ-doped pentacene is rationalized in terms of carrier transport in organic versus inorganic materials. In a typical inorganic semiconductor exhibiting band transport, the carrier released from a dopant is highly delocalized at room temperature with a large inelastic mean free path, e.g., 100 Å in silicon.[23] Thus in STM, only the negatively ionized acceptor remains during imaging. In organic films, on the other hand, room-temperature transport is dominated by hopping, a thermally activated process due to significantly stronger carrier localization, which is why carrier mobilities in organic semiconductors are orders of magnitude smaller than in inorganic semiconductors.[24] It is therefore likely that in an organic film, in the presence of an ionized acceptor molecule, a hole carrier will be localized. Such a carrier trapping process has been discussed previously for doped, disordered organic films[25,26] but has never been observed by STM in any organic system, disordered or otherwise. We thus propose that the subsurface positive charge observed by STM in the pentacene–F_4-TCNQ system is actually a hole localized near an ionized acceptor molecule. The explanation given for the subsurface dopant does not contradict the surface acceptor images (Fig. 2), which reflect a negative charge. In the surface dopant case, the released hole is masked by the Coulomb potential of the ionized acceptor, thus leaving the negatively charged F_4-TCNQ molecule exposed in STM imaging. Indeed, we have taken STS data [Fig. 2(b) inset] on pentacene molecules adjacent to a surface dopant feature (red curve) and on pentacene molecules far from a surface dopant feature (black curve). The DOS in these two cases show no significant shift, as would be expected if the hole is masked

by the Coulomb potential of the ionized acceptor.

In Fig. 4, the fact that the donated hole is observed in STM without signature of the subsurface ionized acceptor can be understood by considering that each presented image was recorded at room temperature over approximately 15 min. Marcus theory gives the intermolecular hopping rate of charge as $\kappa=(t^2/\hbar)(\pi/\lambda k_B T)^{1/2}\exp(-\lambda/4k_B T)$, where t is the transfer integral between neighboring molecules and λ is the reorganization energy.[27] Both quantities have been calculated for all nearest neighbor pairings in crystalline pentacene,[28,29] and lead to a room-temperature hopping rate in the range of 10^{8-13} s^{-1}. Therefore, while the acceptor impurity donates only one hole to the lattice, this hole hops between neighboring molecules while still localized in the vicinity of the ionized dopant. On the (comparatively very slow) time scale of STM scanning, the effect is one of an "average hole" spread over several molecular sites, as illustrated in Fig. 5(c). As STM is exponentially sensitive to tip-sample distance, the STM images reflect only this average hole in the topmost molecules, and not the underlying ionized dopant. The situation at low temperatures may be significantly different, but could not be probed here because of experimental limitations.

DOS plots extracted from STS spectra measured on the pentacene/F_4-TCNQ/pentacene film and are shown in Fig. 5(d). The spectra were recorded with the tip in two distinct positions: (1) over the center of a hillock/depression subsurface dopant feature (red curve), and (2) far from the spatial extent of said dopant feature (black curve). Note that all spectra are taken over pentacene molecules, but the former are influenced by a subsurface dopant. The DOS of pentacene in the presence of a subsurface dopant is shifted by about 0.25 eV to lower energy with respect to the "intrinsic" pentacene DOS, which reflects the potential energy lowering at the surface due to the localized hole, as described above. The spectra also agree with the bias dependence of the hillock/depression feature of Figs. 4(a) and 4(b) as the DOS of pentacene affected by a subsurface dopant is greater for positive bias and lower for negative bias as compared to the intrinsic pentacene DOS. While the exact potential energy shift here depends on many factors, such as relative permittivity and temperature, the STS spectra substantiate the claim that, in a molecular film, the hole released by a subsurface acceptor impurity is localized. Certainly, the donated hole still contributes to transport current in an applied field, as mentioned in the introduction, but it is not highly delocalized as in inorganic semiconductors.

IV. SUMMARY

In our investigation of F_4-TNCQ-doped pentacene, we have presented an STM study of molecular dopants in organic films. Surface F_4-TCNQ molecules diffuse into pentacene vacancies and appear negatively charged, as expected for ionized acceptors, and their bias-dependent behavior is well explained based on DFT calculations of the ionized dopant density of states. Subsurface dopants, however, exhibit the characteristics of positively charged species. This is attributed to the hole donated to the lattice, which remains localized near the dopant at equilibrium, and is spread over several molecular sites. The corresponding positive charge masks the effects of the underlying dopant in STM images. STS spectra show potential-energy lowering of pentacene near a subsurface dopant, in agreement with the proposed model. These results provide molecular-scale visualization of the localization of donated carriers in organic molecular doping.

ACKNOWLEDGMENTS

Financial support from ASEE NDSEG and the National Science Foundation (Grant No. 0705920) are gratefully acknowledged. Many thanks are due to X. Y. Zhu and to M. Muntwiler for valuable discussions on Si(111)/Bi(001)/pentacene sample preparation.

*Corresponding author; sieuh@princeton.edu

[1] J. Blochwitz, M. Pfeiffer, T. Fritz, and K. Leo, Appl. Phys. Lett. **73**, 729 (1998).
[2] W. Gao and A. Kahn, Appl. Phys. Lett. **79**, 4040 (2001).
[3] G. Parthasarathy, C. Shen, A. Kahn, and S. R. Forrest, J. Appl. Phys. **89**, 4986 (2001).
[4] J. Drechsel, B. Männig, F. Kozlowski, D. Gebeyehu, A. Werner, M. Koch, K. Leo, and M. Pfeiffer, Thin Solid Films **451-452**, 515 (2004).
[5] K. Walzer, B. Maennig, M. Pfeiffer, and K. Leo, Chem. Rev. (Washington, D.C.) **107**, 1233 (2007).
[6] A. R. Murphy and J. M. J. Frechet, Chem. Rev. (Washington, D.C.) **107**, 1066 (2007).
[7] W. Gao and A. Kahn, J. Appl. Phys. **94**, 359 (2003).
[8] N. Koch, A. Kahn, J. Ghijsen, J. J. Pireaux, J. Schwartz, R. L. Johnson, and A. Elschner, Appl. Phys. Lett. **82**, 70 (2003).
[9] K. Harada, M. Riede, K. Leo, O. R. Hild, and C. M. Elliott, Phys. Rev. B **77**, 195212 (2008).
[10] Data to be published elsewhere.
[11] J. T. Sadowski, T. Nagao, S. Yaginuma, Y. Fujikawa, A. Al-Mahboob, K. Nakajima, T. Sakurai, G. E. Thayer, and R. M. Tromp, Appl. Phys. Lett. **86**, 073109 (2005).
[12] M. Muntwiler, Q. Yang, W. A. Tisdale, and X. Y. Zhu, Phys. Rev. Lett. **101**, 196403 (2008).
[13] S. D. Ha, Q. Zhang, S. Barlow, S. R. Marder, and A. Kahn, Phys. Rev. B **77**, 085433 (2008).
[14] I. Horcas, R. Fernández, J. M. Gómez-Rodriguez, J. Colchero, J. Gómez-Herrero, and A. M. Baro, Rev. Sci. Instrum. **78**, 013705 (2007).
[15] C. Wagner, R. Franke, and T. Fritz, Phys. Rev. B **75**, 235432 (2007).
[16] R. G. Endres, C. Y. Fong, L. H. Yang, G. Witte, and C. Wöll, Comput. Mater. Sci. **29**, 362 (2004).
[17] J. A. Kubby and J. J. Boland, Surf. Sci. Rep. **26**, 61 (1996).

[18] Z. G. Soos, Annu. Rev. Phys. Chem. **25**, 121 (1974).
[19] S. Braun and W. R. Salaneck, Chem. Phys. Lett. **438**, 259 (2007).
[20] F. Jackel, U. G. E. Perera, V. Iancu, K. F. Braun, N. Koch, J. P. Rabe, and S. W. Hla, Phys. Rev. Lett. **100**, 126102 (2008).
[21] C. Domke, P. Ebert, M. Heinrich, and K. Urban, Phys. Rev. B **54**, 10288 (1996).
[22] R. de Kort, M. C. M. M. van der Wielen, A. J. A. van Roij, W. Kets, and H. van Kempen, Phys. Rev. B **63**, 125336 (2001).
[23] L. Weber and E. Gmelin, Appl. Phys. A: Mater. Sci. Process. **53**, 136 (1991).
[24] G. Malliaras and R. Friend, Phys. Today **58** (5), 53 (2005).
[25] Y. Shen, K. Diest, M. H. Wong, B. R. Hsieh, D. H. Dunlap, and G. G. Malliaras, Phys. Rev. B **68**, 081204(R) (2003).
[26] V. I. Arkhipov, P. Heremans, E. V. Emelianova, and H. Bässler, Phys. Rev. B **71**, 045214 (2005).
[27] R. A. Marcus, Rev. Mod. Phys. **65**, 599 (1993).
[28] Y. Olivier, V. Lemaur, J. L. Bredas, and J. Cornil, J. Phys. Chem. A **110**, 6356 (2006).
[29] W.-Q. Deng and W. A. Goddard, J. Phys. Chem. B **108**, 8614 (2004).